Hydrol. Earth Syst. Sci. Discuss., https://doi.org/10.5194/hess-2018-118
Manuscript under review for journal Hydrol. Earth Syst. Sci.
Discussion started: 27 April 2018

Hydrology and Earth System Sciences
Open Access
Discussions

Discharge hydrograph estimation at upstream-ungauged sections by coupling a Bayesian methodology and a 2D GPU Shallow Water model

Alessia Ferrari[1], Marco D'Oria[1], Renato Vacondio[1], Alessandro Dal Palù[2], Paolo Mignosa[1], and Maria Giovanna Tanda[1]

[1]Department of Engineering and Architecture, University of Parma, Parma, Italy
[2]Department of Mathematical, Physical and Computer Science, University of Parma, Parma, Italy

Correspondence to: Alessia Ferrari (alessia.ferrari@unipr.it)

Abstract. In this paper a novel methodology to estimate the unknown discharge hydrograph at the entrance of a river reach, where no information is available, is presented. The methodology is obtained by coupling an optimization procedure, based on the Bayesian Geostatistical Approach (BGA), with a forward self-developed 2D hydraulic model of the stream. In order to accurately describe the flow propagation in real rivers characterized by large floodable areas, the forward model solves the 2D Shallow Water Equations by means of a Finite Volume explicit shock-capturing algorithm. The forward code exploits the computational power of Graphics Processing Units (GPUs) achieving ratio of physical to computational time up to 1000. With the aim of enhancing the computational efficiency of the inverse estimation, the Bayesian technique is parallelized developing a procedure based on the Secure Shell (SSH) protocol which allows to take advantage of remote High Performance Computing clusters (including those available on the Cloud) equipped with GPUs. The capability of the coupled models is assessed estimating irregular and synthetic inflow hydrographs in real river reaches, taking into account also the presence of downstream corrupted observations. Finally, the capability to adopt this methodology for real cases is demonstrated by reconstructing a real flood wave in a river reach located in Northern Italy.

1 Introduction

The definition of discharge hydrographs in specific river sections is still a relevant hydraulic problem not only for flood modelling purposes, but also for more practical issues related to flood protection measures, hydropower plants, water resource management, design of new structures, etc. Flood routing techniques, either hydrological or hydraulic, are extensively studied and widely used to estimate discharge hydrographs in downstream ungauged sites based on data available at upstream gauged stations (forward propagation). However, often, the flow hydrograph is required in a river section which is completely ungauged and does not have upstream useful information for its definition. In these cases, discharge hydrographs at specific sites can be estimated by coupling rainfall-runoff and forward flood propagation models. However, rainfall-runoff models (Beven (2011)) present several uncertainties associated, for example, with the choice of the model for the basin schematization, with the evaluation of the effective rainfall, and with the calibration procedure. An alternative approach is to assess the upstream unknown flow hydrograph using only the information, in terms of discharge values or water levels, available downstream the selected site and, possibly, the characteristics of the river reach. In literature, this approach is known as reverse flow routing (D'Oria and Tanda (2012)), an ill-posed inverse problem that presents three main challenges: the solution may not exist, or it may be non-unique, and instabilities may arise during the inversion. The traditional attempts of solving the reverse flow routing problem are based on two main approaches: the solution of a reverse form of the Saint Venant equations (e.g. Eli et al. (1974), Szymkiewicz (1993), Dooge and Bruen (2005), Bruen and Dooge (2007)) and the back oriented application of hydrological routing schemes (e.g. Das (2009), Koussis et al. (2012), Koussis and Mazi (2016)). Beyond the approximations introduced by the hydrological routing schemes, the above procedures were applied to simplified reach geometries and flow conditions. In almost all cases, especially considering downstream information affected by errors, instabilities and spurious oscillations appeared; low-pass filters, with subjective parameters, were sometime used to damp the estimated inflow fluctuations. D'Oria and Tanda (2012) and Zucco et al. (2015) provide additional references and details on the reverse flow routing problem. In addition to the above procedures, the estimation of an unknown upstream flow hydrograph, based only on downstream information (observations), can be performed via optimization methods. These techniques aim at finding the upstream flow hydrograph that, routed downstream, best matches the available observations. D'Oria and Tanda (2012) solved the reverse flow routing problem adopting a novel Bayesian Geostatistical Approach (BGA) as optimization procedure, which considers a flow hydrograph as a statistical continuous random function that presents autocorrelation and accounts for uncertainties. The Authors showed the capability of the BGA methodology, in combination with a forward hydraulic model, to estimate the discharges in an upstream ungauged section based only on an available downstream flow hydrograph: the procedure evidenced no instabilities, also in presence of corrupted downstream flow values. The forward model, which solves the 1D Saint Venant equations, was considered already implemented and calibrated and able to describe, with sufficient accuracy, the hydraulic routing process. The BGA method was further extended in order to adopt, as downstream observations, stage hydrographs instead of discharge ones (D'Oria et al. (2014)). Saghafian et al. (2015) identified the upstream hydrograph of a river reach, given the downstream one, by using a Genetic Algorithm coupled with a forward hydraulic model, which solves the 1D Saint-Venant equations under the kinematic wave approximations. Only some minor oscillations and instabilities occurred during the inversion, but the Authors applied the procedure to a rectangular prismatic channel and no errors were added to the downstream observations. Zucco et al. (2015) investigated the reverse flow routing process in natural channels, and estimated the discharge hydrograph in ungauged sections, by means of a Genetic Algorithm coupled with a simplified routing model. The parametric forward model was based on the continuity equation written in a characteristic form, lumped over the entire river reach, and on simplified rating curves at the channel ends. In addition, the unknown inflow hydrograph was assumed distributed in time as a Pearson type III function with three parameters, preventing the possibility of estimating of real flood waves with irregular shapes (e.g. multi-peak hydrographs).

All the previously cited works adopted 1D hydraulic models or simplified hydrological routing models, in combination with different optimization procedures. Nevertheless, in many real cases, the complex hydrodynamic field generated by the flood propagation cannot be accurately described under 1D assumptions and it is necessary to adopt schemes based on the 2D Shallow Water Equations, even if this poses the drawback of the computational efficiency and requires a detailed terrain survey.

However, nowadays, bathymetric data can be easily obtained from high-resolution Digital Terrain Models (DTM) and fast 2D numerical models have been developed. With the purpose of estimating the discharge hydrograph in an upstream ungauged river section, having water level information only in a downstream observation site, this paper extends the BGA methodology for reverse flow routing of D'Oria and Tanda (2012) and D'Oria et al. (2014) to 2D forward modelization in order to model natural rivers with complex geometry, including flood plains and floodable areas. With this aim, the stable, accurate and fast PARFLOOD GPU code (Vacondio et al. (2014),Vacondio et al. (2017),Vacondio et al. (2016)), which solves the conservative form of the 2D Shallow Water Equations on a finite volume scheme, is adopted as forward model and coupled to the inverse estimation procedure. In order to reduce the computational times, the Jacobian matrix estimation procedure, which is the key point of the BGA method, has been parallelized. Additionally, a host-server data management procedure has been implemented so as to exploit the computational power of remote large modern supercomputer and or cloud HPC resources. The capability of the optimization procedure has been tested by estimating real or pseudo real inflow hydrographs in natural river reaches, where 1D models cannot accurately describe the flood propagation. Moreover, during the discharge estimation, the presence of downstream corrupted observations has also been taken into account, since registered data at gauging stations are quite often affected by instrumental errors. Dealing with real recorded data and real field application, the discharge parameter values have been estimated in a logarithmic space, in order to prevent the rise of negative values.

The paper is organized as follows: in Sect. 2 the theory of the Bayesian Geostatistical Approach is illustrated. A step-by-step description of the inverse procedure is provided in Sect. 3: the parallel implemented scheme, the forward model optimization for reducing the run times and the iteration management between the local host and the remote server are detailed described. Section 4 is dedicated to the procedure validation, which concerns the estimation of inflow hydrographs with different shapes in two rivers in Northern Italy. The application of the inverse procedure for reconstructing a historical flooding event is presented in Sect. 5. Some concluding remarks are finally outlined in Sect. 6.

2 Theory of the Bayesian Geostatistical Approach

The optimization software adopted to solve the reverse flow routing problem is the bgaPEST (Fienen et al. (2013)), which implements the Bayesian Geostatistical Approach of Kitanidis (1995) and it is developed according to the PEST (Model Independent Parameter Estimation) parameter estimation software (Doherty (2016)). The bgaPEST is appropriate to solve inverse problems (in a context of a highly parametrized inversion), which are characterized by unknown parameters that are correlated one another in space or time, as for example the discharge values of a flow hydrograph. The first applications of the inverse methodology are related to the estimation of spatial parameter fields in a groundwater context (Kitanidis and Vomvoris (1983), Hoeksema and Kitanidis (1984), among others) but later the method has been adopted to evaluate unknown time functions in different areas (e.g. Snodgrass and Kitanidis (1997), Michalak et al. (2004), Butera et al. (2013), D'Oria and Tanda (2012), D'Oria et al. (2015), Leonhardt et al. (2014)).

Hydrol. Earth Syst. Sci. Discuss., https://doi.org/10.5194/hess-2018-118
Manuscript under review for journal Hydrol. Earth Syst. Sci.
Discussion started: 27 April 2018

Hydrology and Earth System Sciences
Open Access
Discussions

2.1 The Bayes' theorem

The crux of the adopted bgaPEST, as well as other methods based on the Bayesian Approach, is the Bayes' theorem, which reads:

$$p(\mathbf{s}|\mathbf{y}) \propto L(\mathbf{y}|\mathbf{s})\, p(\mathbf{s}) \tag{1}$$

where **s** is the vector of the unknown parameters, **y** is the vector of the measured data, $p(\mathbf{s}|\mathbf{y})$ is the posterior probability density function (pdf) of **s** given **y**, $L(\mathbf{y}|\mathbf{s})$ is the likelihood function and p(**s**) is the prior probability density function of **s**. Since the present work aims at estimating an upstream hydrograph in an ungauged section, assuming the knowledge of downstream water levels, **s** represents the discharge values over time of the unknown inflow hydrograph, whereas **y** denotes the downstream water level observations. Following Eq.(1), the posterior pdf, which represents the parameter knowledge after the observations, can be seen as a combination between a priori knowledge on the parameters (prior pdf), where a priori means that the observed data are still not considered, and information about parameters contained in the measured data (likelihood function) (Glickman and Van Dyk (2007)). In the BGA method proposed by Kitanidis (1995), the prior pdf and the likelihood function are described by means of Gaussian distributions and the best set of parameter **s** is obtained by maximizing the posterior pdf.

2.1.1 The likelihood function

Focusing on the terms of the Bayes' theorem in Eq.(1), the likelihood function $L(\mathbf{y}|\mathbf{s})$, characterizes the misfit between observed data and model results (Fienen et al. (2013)). Starting from the results of the forward model, $L(\mathbf{y}|\mathbf{s})$ delineates how a particular set of parameters **s** is able to reproduce the observations **y** in space and/or time, therefore accounting for the epistemic errors. The investigated inverse problem presents different sources of errors, which are related to the conceptual schematization of the inverse procedure, to the numerical forward model and to the data measurement. In the likelihood function, the errors are assumed to be independent and identically distributed, with null mean and covariance matrix, expressed as follows:

$$\mathbf{R} = \sigma_R^2 \mathbf{I} \tag{2}$$

where σ_R^2 denotes the variance that regulates the misfit between observed and modeled data, and **I** the identity matrix.

2.1.2 The prior probability density function

The prior knowledge about **s** (p(**s**) in Eq.(1)) is limited to the assignment of a mean value (unknown and estimated during the procedure) and a characteristic about continuity and/or smoothness implemented as covariance matrix. It furnishes a soft knowledge about the structure/shape of the unknowns and provides a regularization of the solution; the prior can also be used to enforce non-negativity to the parameters (D'Oria and Tanda (2012)). The prior mean is defined as:

$$E[\mathbf{s}] = \mathbf{X}\boldsymbol{\beta} \tag{3}$$

Hydrol. Earth Syst. Sci. Discuss., https://doi.org/10.5194/hess-2018-118
Manuscript under review for journal Hydrol. Earth Syst. Sci.
Discussion started: 27 April 2018

where E is the expected value, $\boldsymbol{\beta}$ is the vector of drift coefficients (a single value in this case), and $\mathbf{X}$ is a known matrix of basis functions (a single vector of ones, in this case), which link each value of $\mathbf{s}$ with the appropriate element of $\boldsymbol{\beta}$ (Fienen et al. (2008)).

The prior covariance matrix of the unknown parameters $\mathbf{Q}_{ss}$ is then defined as:

$$\mathbf{Q}_{ss} = E\left[(\mathbf{s}-\mathbf{X}\boldsymbol{\beta})(\mathbf{s}-\mathbf{X}\boldsymbol{\beta})^T\right] \quad (4)$$

In the context of geostatistics, the covariance matrix $\mathbf{Q}_{ss}$ is a function of the separation distance (in time in this case) between the parameters and describes their deviations from the mean behavior. Different models can be adopted to describe the covariance; for example, it can be assumed as a linear function, represented through a limiting case of the exponential covariance model (Fienen et al. (2008)), according to the following relation:

$$\mathbf{Q}_{ss}(\theta) = \theta l \exp\left(-\frac{|\mathbf{d}|}{l}\right) \quad (5)$$

where $\mathbf{d}$ represents the vector of the separation distances in time between the parameters, l a fixed integral scale ($l = 10\max(d)$) and θ the slope (structural parameter), which influences the correlation between the discharge values of the unknown hydrograph. A different formulation (D'Oria et al. (2014)) defines the prior covariance matrix $\mathbf{Q}_{ss}$ by means of a Gaussian model characterized by two structural parameters (σ_s^2 and l):

$$\mathbf{Q}_{ss}(\theta) = \sigma_s^2 \exp\left(-\frac{|\mathbf{d}^2|}{l^2}\right) \quad (6)$$

where σ_s^2 denotes the variance. The linear function (Eq.(5)) enforces only continuity to the solution whereas the Gaussian model (Eq.(6)) adds also some degree of smoothness, but the final solution is still driven by the observations.

2.1.3 The posterior probability density function

With the assumptions made, the likelihood and prior terms, that compose the posterior pdf of Eq.(1), can be rewritten as follows (Fienen et al. (2009); D'Oria and Tanda (2012); D'Oria et al. (2014)):

$$L(\mathbf{y}|\mathbf{s}) = \exp\left(-\frac{1}{2}(\mathbf{y}-\mathbf{h}(\mathbf{s}))^T \mathbf{R}^{-1}(\mathbf{y}-\mathbf{h}(\mathbf{s}))\right) \quad (7)$$

$$p(\mathbf{s}) = \exp\left(-\frac{1}{2}(\mathbf{s}-\mathbf{X}\boldsymbol{\beta})^T \mathbf{Q}_{ss}^{-1}(\mathbf{s}-\mathbf{X}\boldsymbol{\beta}))\right) \quad (8)$$

The term $\mathbf{h}(\mathbf{s})$, in the likelihood function, represents the modeled values in the same place and time of the available observations $\mathbf{y}$. Therefore, to evaluate $\mathbf{h}(\mathbf{s})$, a forward model of the considered river reach that is able to describe the hydraulic routing process is required in order to provide, for a given set of parameter $\mathbf{s}$, the corresponding downstream water levels.

Recalling that the aim of the inverse procedure is to obtain the vector of the unknown parameters $\mathbf{s}$, as well as to quantify the uncertainty in the estimation, the solution is found maximizing the posterior pdf. In case a linear relationship between

Hydrol. Earth Syst. Sci. Discuss., https://doi.org/10.5194/hess-2018-118
Manuscript under review for journal Hydrol. Earth Syst. Sci.
Discussion started: 27 April 2018

parameters and observations (linear forward model) holds, the best estimate $\hat{\mathbf{s}}$ of vector $\mathbf{s}$ (and $\hat{\beta}$ of β) is obtained by solving the following linear system of equations (Michalak and Kitanidis (2003)):

$$\begin{cases} \hat{\mathbf{s}} = \mathbf{X}\hat{\boldsymbol{\beta}} + \mathbf{Q}_{ss}\mathbf{H}^T\boldsymbol{\xi} \\ \begin{bmatrix} \mathbf{H}\mathbf{Q}_{ss}\mathbf{H}^T + \mathbf{R} & \mathbf{H}\mathbf{X} \\ \mathbf{X}^T\mathbf{H}^T & 0 \end{bmatrix} \begin{bmatrix} \boldsymbol{\xi} \\ \hat{\boldsymbol{\beta}} \end{bmatrix} = \begin{bmatrix} \mathbf{y} \\ 0 \end{bmatrix} \end{cases} \tag{9}$$

where $\mathbf{H}$ is the sensitivity (Jacobian) matrix, representing how the observations $\mathbf{y}$ are influenced by a single unknown parameter s_i (D'Oria et al. (2015)). However, for this particular problem, $\mathbf{h(s)}$ is nonlinear and therefore matrix $\mathbf{H}$ depends on $\mathbf{s}$. Following the quasi-linear geostatistical approach (Kitanidis (1995)), for each iteration k, the relationship between observations and parameters is successively linearized about a candidate solution $\mathbf{s}_k$:

$$\mathbf{h(s)} \approx \mathbf{h}(\mathbf{s}_k) + \widetilde{\mathbf{H}}_k(\mathbf{s} - \mathbf{s}_k) \tag{10}$$

and then a correction to the measurements is applied according to the following relation:

$$\mathbf{y}_k = \mathbf{y} - \mathbf{h}(\mathbf{s}_k) + \widetilde{\mathbf{H}}_k\mathbf{s}_k \tag{11}$$

Therefore, the sensitivity matrix is evaluated at each iteration, as follows (D'Oria et al. (2014)):

$$\widetilde{\mathbf{H}}_k = \left.\frac{\partial\mathbf{h(s)}}{\partial\mathbf{s}}\right|_{\mathbf{s}_k} \tag{12}$$

Analogously to the linear system in Eq. (9), the linearized system is solved according to:

$$\begin{bmatrix} \widetilde{\mathbf{H}}_k\mathbf{Q}_{ss}\widetilde{\mathbf{H}}_k^T + \mathbf{R} & \widetilde{\mathbf{H}}_k\mathbf{X} \\ \mathbf{X}^T\widetilde{\mathbf{H}}_k^T & 0 \end{bmatrix} \begin{bmatrix} \boldsymbol{\xi}_{k+1} \\ \hat{\boldsymbol{\beta}}_{k+1} \end{bmatrix} = \begin{bmatrix} \mathbf{y}_k \\ 0 \end{bmatrix} \tag{13}$$

and the next estimate of the parameters is evaluated by means of:

$$\widetilde{\mathbf{s}}_{k+1} = \mathbf{X}\hat{\boldsymbol{\beta}}_{k+1}\mathbf{Q}_{ss}\widetilde{\mathbf{H}}_k^T\boldsymbol{\xi}_{k+1} \tag{14}$$

A proper selection of the covariance model structural parameters (θ, σ_s^2 and l) and optionally of the epistemic error variance σ_R^2 is important to reach a good solution. However, the structural parameters are estimated from the data using a Bayesian adaptation of the Restricted Maximum Likelihood (RML) method of Kitanidis (1995), which adopts probability functions and allows reaching the best compromise between the fitting of the modeled data and the observations, and the prior information (Fienen et al. (2013)). Dealing with non linear problems, unknown ($\mathbf{s}$) and structural parameters must be iteratively estimated in successive steps.

Finally, at the end of the estimation, the linearized uncertainties of the unknowns can be evaluated in terms of the posterior covariance matrix of the estimated parameters (D'Oria et al. (2014)). The diagonal of this matrix represents the variance related to the parameter estimation that allows defining the 95% credibility interval of the resulted parameters.

3 Description of the Bayesian estimation procedure

After having described the theory of the Bayesian approach in Sect. 2, some operational information about the BGA inverse procedure is now illustrated. As mentioned in the Introduction and sketched in Fig. 1-a, the goal of the adopted BGA methodology is the estimation of the discharge hydrograph in an upstream-ungauged river section (identified by a question mark in Fig. 1-a), having information about water levels observed in a downstream section (intermediate site in Fig. 1-a). A boundary condition, downstream of the observation site, must also be specified; this can be based on observed data or can be approximated extending the computational domain faraway from the intermediate section. The inverse method estimates N_p parameters (the vector of the unknown parameters **s** in Eq. (1)), which derive from the discretization of the discharge hydrograph by means of time intervals, regular in this case (Fig.1-b).

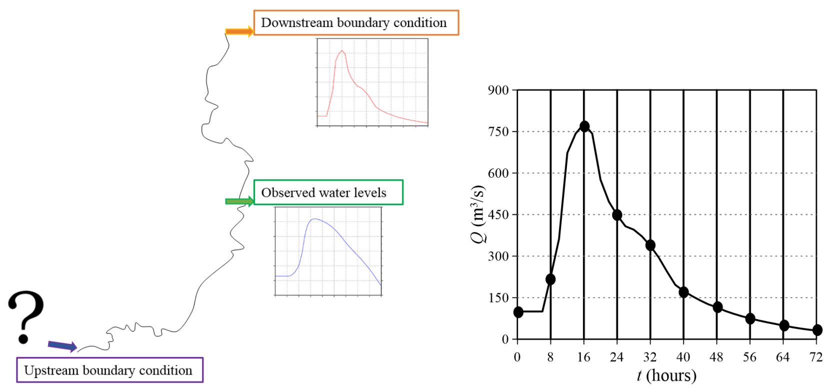

(a) (b)

Figure 1. Definition of the reverse flood routing problem (a) and of the unknown parameters (b).

The BGA algorithm solves the inverse problem by means of the following steps.

Firstly, the unknown parameters and the structural ones are initialized. The first ones may be all assumed equal to a constant value coherent with the considered river, whereas the structural parameters are usually set as to guarantee a flat solution (complexity is introduced during the optimization process only if supported by the data) and the variance of the epistemic errors is assumed close to the expected one.

Assuming the first guess of the unknown parameters as upstream boundary condition, the hydraulic forward model is run and the resulted water levels are extracted at the observation site. The simulation of a base run, once assumed a particular set of parameters (deriving from the initialization or from previous estimation steps), represents a mandatory step for the Jacobian/sensitivity matrix evaluation, which is performed at this point of the procedure. The Jacobian matrix quantifies how each observation is influenced by the variation of each estimable parameter, and it is calculated using a finite differences method. According to Eq. (12), each element is evaluated as the ratio between the variation of each observation for given variation of each parameter (numerator) and the variation of the parameter value with reference to the base run (denominator). Therefore, additionally to the base run, the hydraulic forward model is further run as many times as the number of parameters to estimate N_p. At each run, a single value of the upstream boundary condition is modified by a known quantity with respect to the previous value (denominator of Eq. (12)), and the hydraulic forward model is run. Therefore, each simulation tests the sensitivity of the resulted water levels (all the observations at once) to the variation of a single parameter *i*.

In order to exemplify this step, Fig. 2-a shows the discharge imposed as upstream boundary condition for a base run: after the propagation, the resulted water levels extracted at the observation site are shown in Fig. 2-c. Assuming that the Jacobian matrix is testing the sensitivity to parameter *i*, in Fig. 2-b the considered parameter is varied with a known quantity and a new upstream boundary condition is defined (solid line); it is worth noting that the solid and the dotted lines differ only for the parameter *i*. The water levels resulted from this single parameter variation are shown in Fig. 2-d (solid line): they are identical to the base run ones until time *i*-1, whereas after they differ from those of the base run (dotted line). The computation of the differences between the resulted water levels of the simulation *i* and of the base run (solid and dotted lines) and the variation of parameter *i* allows computing the column *i* of the Jacobian matrix, which is a $N_{obs}\times N_p$ matrix, where N_{obs} represents the number of the observations.

After having collected all the perturbed observations, the Jacobian/sensitivity matrix is evaluated and a new set of parameters **s** is estimated (Eq. (14)).

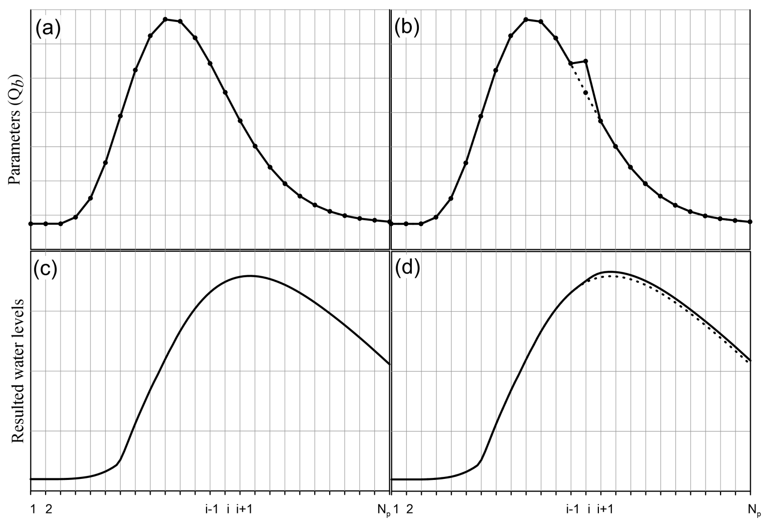

Figure 2. Example of the base run (a) and of the run *i* for the Jacobian matrix evaluation (b).

Then the first set of resulted parameters is used for evaluating a new Jacobian matrix and as a result, a second set of parameters is estimated. This procedure is repeated until the convergence or the maximum number of iteration N_i is reached. Then, holding the last set of parameters **s** constant, the structural parameters are estimated. Due to the non-linearity of the problem, the model and the structural parameter estimation is repeated until convergence of the lasts (or the maximum number of iterations N_o is reached). Therefore, the BGA implementation requires running the forward model N_t times, according to

Hydrol. Earth Syst. Sci. Discuss., https://doi.org/10.5194/hess-2018-118
Manuscript under review for journal Hydrol. Earth Syst. Sci.
Discussion started: 27 April 2018

Hydrology and Earth System Sciences Open Access Discussions

the following relation (Fienen et al. (2013)):

$$N_t = (N_p + 1)\, N_o N_i + 1 \tag{15}$$

The whole BGA procedure previously described is sketched in Fig. 3-a.

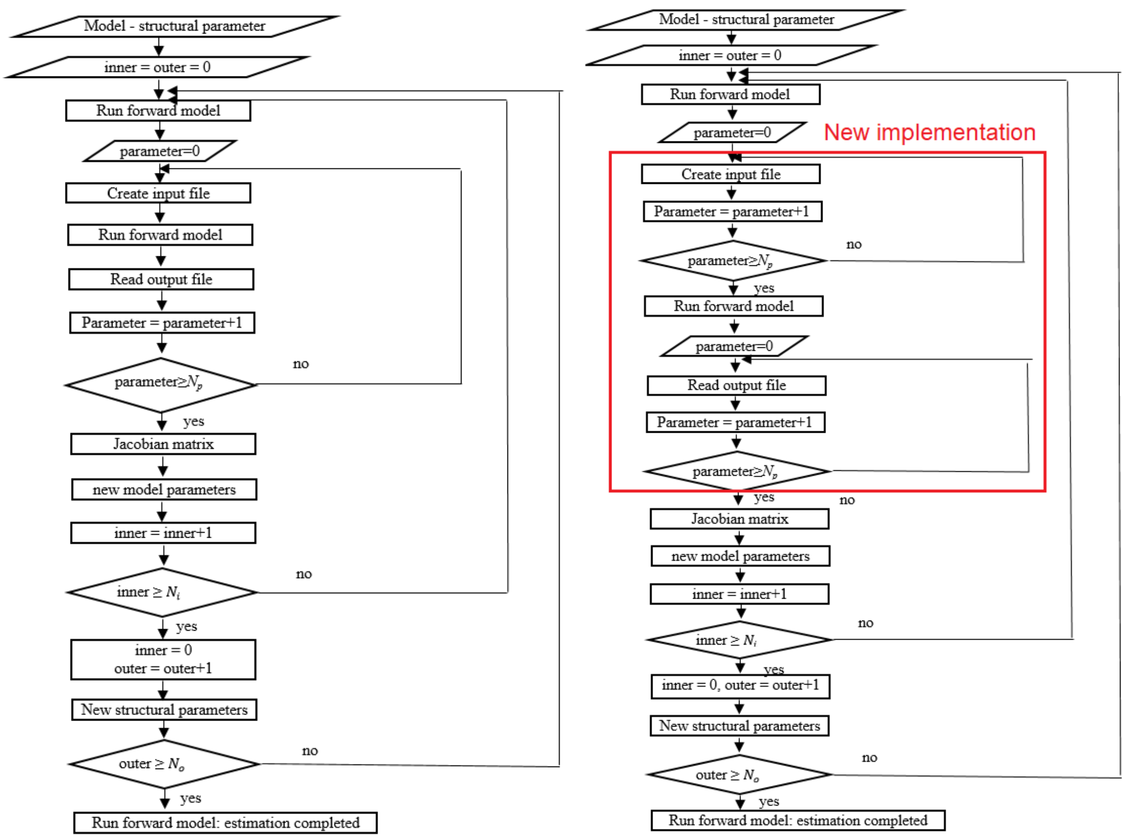

(a) (b)

Figure 3. Scheme of BGA algorithm in the serial (a) and parallel (b) version.

3.1 Parallelization of the Jacobian matrix evaluation

Focusing on the total computational time required by the inverse estimation procedure, it emerges that the most relevant contribution is ascribed to the run of the forward model, rather than to the bgaPEST operations (i.e. the computation of each element of the Jacobian matrix). However, since each N_p run in Eq. (15) checks the sensitivity of the observations to the variation of a single parameter, the solution of a test does not have effects on the solution of the other ones. Therefore, in order to reduce the computational burden, the independent N_p runs can be potentially performed in parallel.

In this work, the PARFLOOD 2D-GPU numerical model presented in Vacondio et al. (2014) and Vacondio et al. (2017) has been adopted for routing the inflow hydrograph. Therefore, the bgaPEST routine to evaluate the Jacobian matrix has been parallelized in order to run simulations taking advantage of the computational capability of modern High Performance Computing (HPC) clusters, which are usually equipped with many GPUs. The implemented parallel procedure, which is sketched in the flow chart of Fig. 3-b, handles the parallelism among host and GPUs by means of the Secure Shell network protocol (SSH) and manages the most operative parts of the parallelism (login, run, etc.) outside the bgaPEST code. In the serial version (Fig. 3-a), the crucial part of the implementation consists in a do-loop over the parameters. Considering an i parameter, firstly the input file that will be read by the forward model is written, then the model is run and finally the resulted values are read. In the modified version (Fig. 3-b), this main loop is split in three parts: firstly, all the input files (equal to N_p), inside of which a particular parameter is modified are written, then the forward model is run, and finally a second loop is performed to read all the resulted values.

3.2 The forward model

In the parallel bgaPEST (Fig. 3-b), the "Run forward model" instruction actually runs a shell script, which controls the file transfer between the host (a classical PC or a single node of a cluster), and the HPC platform, the creation of the N_p simulations for the Jacobian matrix evaluation, and the run of the 2D-SWE GPU code on the device (GPU). In the present work, a cluster with 10 NVIDIA ® Tesla ® P100 GPUs hosted by the University of Parma was adopted. As shown in Fig. 4, the bgaPEST algorithm runs on the CPU of a computer, where the N_p simulations (in Fig. 4 assumed equal to three for the sake of simplicity) are firstly created and then sent to the server user partition, by means of the SSH protocol. Here, the cluster access node schedules all the jobs submitted by the users, using the HPC scheduler Portable Batch System (PBS). Then, each simulation is assigned to a specific GPU node. At the end of the computation, the observations are extracted and the output files remain on the cluster partition, until the CPU verifies via SSH the end of the simulation and copies the results back. The procedure sketched in Fig. 4 and following described represents one of the N_t iterations.

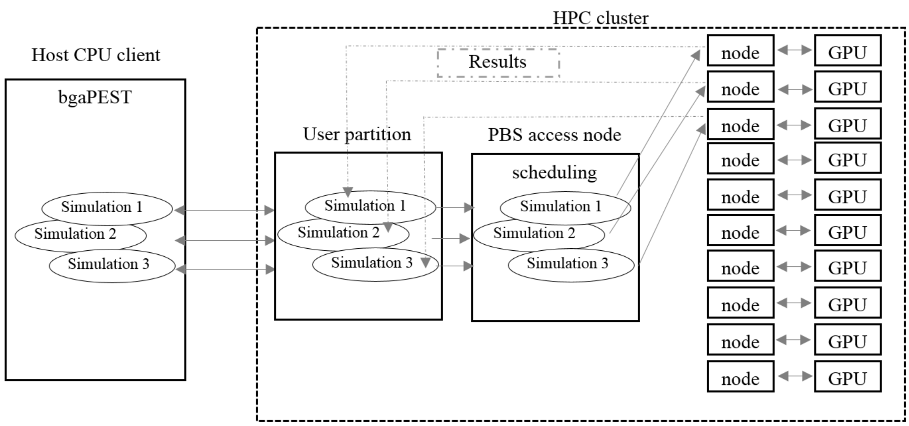

Figure 4. Schematization of the data transfer assuming three parameters and thus three parallel simulations.

With the aim of describing in detail the "Run forward model", after having clarified the data transfer procedure (Fig. 4), in Listing 1 the structure of the shell file is presented. In order to use the Algorithm for different test cases and potentially on different HPC clusters, all the paths are firstly declared together with the involved variables (number of parameters to estimate, time interval among parameters, start/end of the simulation) (line 2). Then, the algorithm (line 3) checks if the considered run is one useful for the Jacobian matrix evaluation, where a given parameter varies, or if it is the base run. Considering the first if condition true (line 3), the script generates and copies all the simulations to the server (lines 5-7). These tests contain the same bathymetrical, initial conditions (water level and velocity), roughness configuration but different upstream boundary condition; each simulation tests the sensitivity to the variation of a given model parameter. Moreover, all the simulations adopt the same grid (Cartesian or multiresolution), which is generated only once at the beginning of the procedure. It is relevant to notice that all the N_p simulations have not to be run from time t_{start} to time t_{end}. In effect, the variation of parameter i causes effects only after time t_i and thus the results until t_i are still identical to the base run (see Fig. 2). The PARFLOOD model guarantees the possibility of using the results of the base run and starting simulations from time t_i. The theoretical physical time T of simulations run from time t_{start} to time t_{end} is evaluated as follows:

$$T = N_p\,(N_p - 1)\,\Delta t \qquad (16)$$

where N_p denotes the parameter number and Δt the time interval between parameters i and $i+1$.

Conversely, the physical time T^* of simulations run from time $t_{restart}$ to time t_{end} reads:

$$T^* = (N_p - 1)\Delta t + \sum_{i=2}^{N_p} \left[N_p - (N_i - 1)\right]\Delta t \qquad (17)$$

As pointed out by Eq. (16)-(17) and exemplified in Fig. 5 for a test case with 20 parameters, this simply operation allows reaching a relevant decrease of the total computational times. Therefore, at line 8, the algorithm computes the time useful to restart the simulation.

In order to perform the simulation, the host logins to the HPC cluster server by means of the SSH protocol (line 9) and a sleep condition ensures the login procedure (line 10). Then the job is submitted to the queue of the cluster using external parameters for passing the name of the simulation folder and the time for restart (line 11): the submitted job contains the reference to the PBS queue and the link to the executable 2D-SWE GPU code. At the end of the simulation, the water levels at the observation site are automatically extracted. Once the job is submitted, the SSH login is closed (line 12). After having submitted all the simulations, for each parameter (line 15) the code regularly (line 18) tests via SSH the presence of the end_file, which states the end of the simulation (line 20), and waits in case it is missing (line 25). Once the simulation is finished, the resulted observations are copied back to the CPU (line 28) and the folder is removed from the server (line 29).

On the other side, the else condition (line 31) is true for the base run, which is necessary for the Jacobian matrix computation. The simulation folder, which contains all the necessary input files, is copied to the server (line 32) and the job is submitted (line

Hydrol. Earth Syst. Sci. Discuss., https://doi.org/10.5194/hess-2018-118
Manuscript under review for journal Hydrol. Earth Syst. Sci.
Discussion started: 27 April 2018

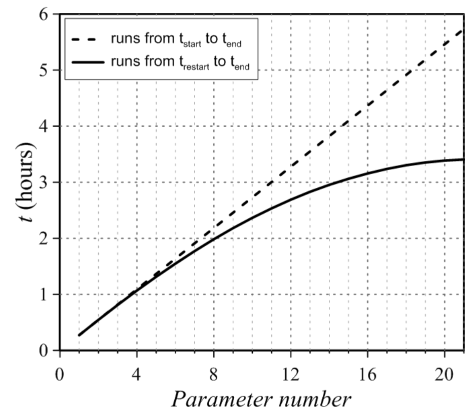

Figure 5. Comparison of the cumulative computational times obtained simulating the N_p runs from time t_{start} until t_{end} or with restart options.

35). Then, the algorithm periodically verifies the end of the simulation and copies the results back to the CPU (lines 39-49). It is relevant to notice that the base run is firstly performed, whereas the other N_p ones can be parallel performed.

Listing 1. "Run forward model" for the parallel bgaPEST scheme

```
1  #!/bin/bash
2  Variable and path declaration
3  if [parameter run];
4      then
5      for (( i=1; i<=Np; i++ ))
6          do
7            Create and copy the simulation folder to the server (simulation_i)
8            Compute the time from which restarting the simulation
9            ssh server name << EOF
10           sleep 15
11           ssh submission: frame number for restart , name of the test case, job to submit
12           exit
13           EOF
14     done
15     for (( i=1; i<=Np; i++ ))
16         do
17           end_file=0
18           while [ end_file -eq 0 ];
19           do
20           ssh server name  find server_path -iname end_file.txt | wc -l > end_file
21           if [end_file];
22           then
23                continue
24           else
```

```
                sleep 10
            fi
        done
        Copy the file with observation from server to CPU
        Remove the simulation folder on the cluster
else
        Create and copy the simulation folder to server
        ssh server name << EOF
        sleep 15
        ssh submission: frame number for restart , name of the test case, job to submit
        exit
        EOF
        end_file=0
        while [ end_file -eq 0 ];
        do
            ssh server name  find server_path -iname end_file.txt | wc -l > end_file
            if [end_file];
            then
                continue
            else
                sleep 10
            fi
        done
        Copy the file with observation from server to CPU
fi
```

4 Validation of the inverse methodology

With the purpose of validating the BGA method described before, it is worth noting that reference solutions for inverse problems are by definition unavailable, since the goal of the methodology is the estimation of an upstream inflow hydrograph that is unknown at the beginning of the process. Therefore, in this section the inflow hydrographs in two natural rivers in Northern Italy are estimated and the reference solutions, which are necessary in order to validate the inverse procedure, are obtained as follows (D'Oria et al. (2014)). Considering the domain in Fig. 6, a selected inflow discharge Q^{ref} is routed from the upstream section A until the downstream boundary D, where a rating curve is imposed far away from C. The resulted water level hydrograph is extracted in sites B and C. The inverse procedure is then applied to the sub-domain sketched with solid line in Fig. 6, by assuming the water levels in sites B and C (resulted from step 1) as observations and downstream boundary condition, respectively. The methodology estimates the inflow Q^{est} assuming that no information is available on the discharge (or water stage) at the inflow.

Quantitative information about the accuracy of the inverse methodology is here provided evaluating the differences between the reference Q^{ref} and the estimated Q^{est} hydrographs by means of three different indicators. Firstly, the Nash-Sutcliffe

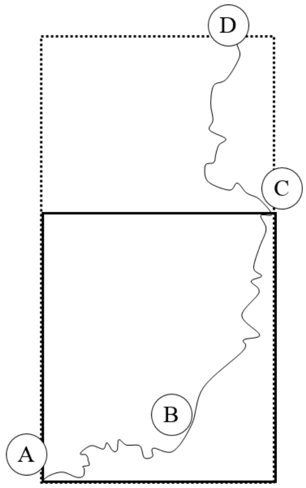

Figure 6. Exemplification of a test case definition.

efficiency criterion (Nash and Sutcliffe (1970)) E_h was adopted, according to the following relation:

$$E_h = \left[1 - \frac{\sum_{i=1}^{N_p}(Q_i{}^{ref} - Q_i{}^{est})^2}{\sum_{i=1}^{N_p}(Q_i{}^{ref} - \overline{Q}^{ref})^2}\right] \cdot 100 \tag{18}$$

where N_p is the number of parameters, Q_i^{ref} and Q_i^{est} are the *i*-th reference and estimated inflow values, respectively, and $\overline{Q}^{ref}$ is the mean value of the reference hydrograph. Then, the root mean square error, RMSE was evaluated as follows:

$$RMSE = \sqrt{\frac{\sum_{i=1}^{N}(Q_i{}^{ref} - Q_i{}^{est})^2}{N_p}} \tag{19}$$

Finally, the error in the peak discharge E_p was assessed as:

$$E_p = \left[\frac{Q_p^{est}}{Q_p^{ref}} - 1\right] \cdot 100 \tag{20}$$

where Q_p^{est} and Q_p^{ref} denote the peak discharge value of the estimated and reference hydrographs, respectively.

4.1 Inflow hydrograph estimation on the Parma River

The first test concerns the estimation of a Synthetic Discharge Hydrograph at the entrance of the Parma River (Northern Italy). Figure 7-a illustrates the studied domain and the locations of the upstream boundary condition A, of the observation site B and of the downstream boundary section C. The domain includes a 20-km long reach, which is characterized by several meanders and flood plains. As shown in Fig. 7, the flow field significantly varies at low and high discharge values due to the river morphology. At the beginning of the flood wave, the flow is characterized by both low water depths (7-b) and velocity (7-d). Conversely, at the arrival of the flood pick, most of the meanders are cut by the flow, as shown in (7-c) and (7-e) for water

Hydrol. Earth Syst. Sci. Discuss., https://doi.org/10.5194/hess-2018-118
Manuscript under review for journal Hydrol. Earth Syst. Sci.
Discussion started: 27 April 2018

Hydrology and Earth System Sciences
Open Access
Discussions

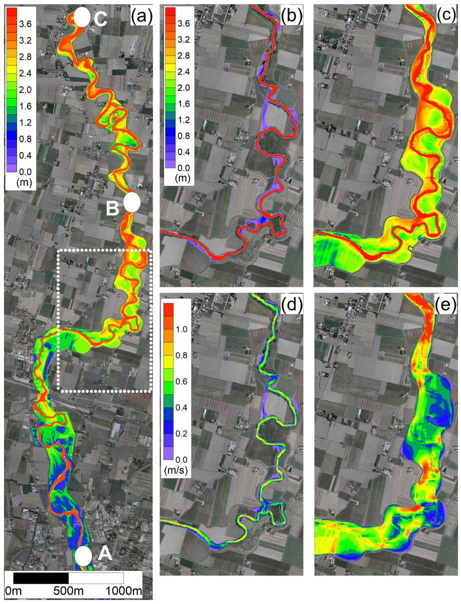

Figure 7. Map of the maximum simulated water depths in the Parma river (a): the upstream (A) and downstream (C) boundary conditions and the intermediate observation site (B) are indicated. With reference to the area marked with dotted white line in (a), (b) and (c) represent the water depths and (d) and (e) the velocity field at low and high discharge values, respectively.

depths and velocity, respectively. This makes the adoption of 1D numerical schemes difficult to accurately describe the flood propagation.

The bathymetry was derived from a 1 m resolution DTM obtained through a LiDAR survey carried out in drought condition. The domain was discretized by means of a Cartesian grid with cell sizes $\Delta x = \Delta y = 4$ m and about $275 \cdot 10^3$ computing cells were adopted. The Manning roughness coefficient was assumed equal to 0.05 s/m$^{1/3}$. The steady state values of water depth and velocity fields obtained considering the initial discharge value of the hydrograph are adopted as initial conditions.

The inflow condition to be estimated concerns a Synthetic Discharge Hydrograph with gamma distribution that was calculated as follows (D'Oria et al. (2015)):

$$Q(t) = A + B \cdot f(t,b,k) \tag{21}$$

where t denotes the time, A the base flow (constant value), B the volume above the base flow (constant value) and f the gamma distribution, which states:

$$f(t,b,k) = \frac{1}{k^b \Gamma(b)} t^{b-1} e^{-\frac{t}{k}} \tag{22}$$

where $\Gamma(b)$ represents the gamma function defined through the parameters b and k that denote the shape and the scale parameter, respectively. The parameters of the gamma distribution were set as follows: A = 100 m^3/s, B =3·10^7 m^3, b = 6 and k = 10000 s. The resulted flood wave presented a peak value of about 630 m^3/s at time (b-1)k = 14 hours (Fig. 8-a).

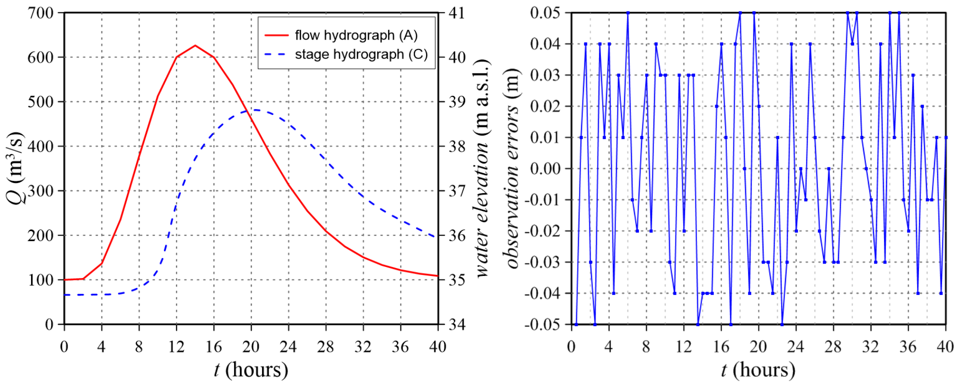

(a) (b)

Figure 8. Parma inflow: flow and stage hydrographs referred to sections A and C, respectively (a) and observation error distribution (b).

During the estimation, when the sensitivity to the first parameter p_1 is investigated, the steady state flow for the initial discharge is also recomputed. This means that parameter p_1 determines not only the first value of the estimated flood wave but also it governs the initial condition of the river reach.

The inflow hydrograph duration was limited to 40 hours and it was discretized using 2 hours steps (N_p=21), whereas the observation stage hydrographs were discretized every 0.5 hours (80 water levels). The prior pdf was defined by means of a Gaussian covariance model, and the initial structural parameters were set as reported in Table 1. In order to avoid non-physical discharge values during the computations, non-negativity was enforced to the unknown parameters performing the estimation in a logarithmic space. The initial model parameter values were defined by applying the linesearch tool of the bgaPEST, which damps the solution between successive iterations (Fienen et al. (2013)), and avoids numerical instabilities that may occur starting from a worse first choice of the parameters.

The inflow hydrograph was estimated firstly considering the observations free of errors and with truncation error resulting in a variance of 10^{-8} m^2. Then, the same discharge hydrograph was defined corrupting the observed water levels with random errors uniformly distributed with maximum deviations of $\pm$0.05 m and variance 10^{-3} m^2 (Fig. 8-b).

Qualitative assessment of the inverse methodology is achieved by comparing the reference with the estimated inflow hydrograph, as well as the observed with the modeled water levels in the observation site. Considering the simulation without errors in the observations, Fig. 9 shows that the estimated flood wave overlaps the reference one (a), and the modeled water levels agree with the measured ones (b). Particularly, with reference to the peak value, the estimated flood wave presents the maximum misfit of 0.2%, whereas the modeled water levels differ from the observed ones less than the 0.01%.

The results of the simulation with random errors corrupting the observations are depicted in Fig. 10. The estimated flood wave well matches the reference one, presenting a misfit referred to the peak value lower than the 5%, and similarly the modeled water levels reproduce the reference ones with residual less than 1%. Only the last value of the reconstructed flood wave it is slightly overestimated, since the more the tested parameter nears the end of the wave, the fewer observations contain infor-

Hydrol. Earth Syst. Sci. Discuss., https://doi.org/10.5194/hess-2018-118
Manuscript under review for journal Hydrol. Earth Syst. Sci.
Discussion started: 27 April 2018

Hydrology and Earth System Sciences
Open Access
Discussions

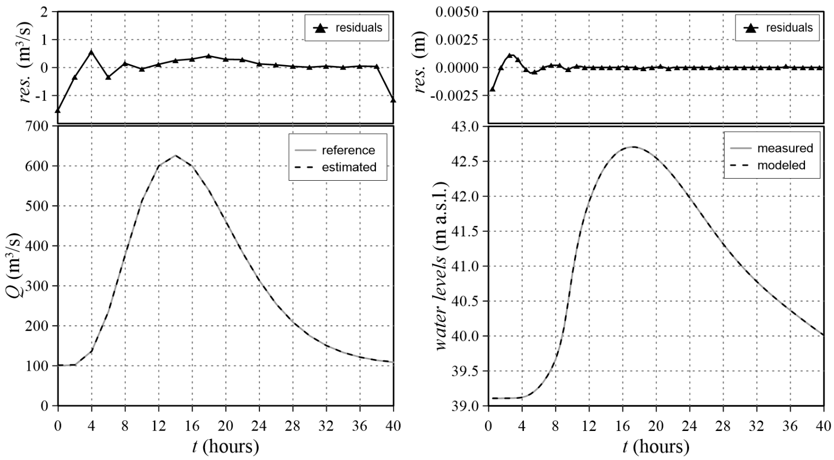

(a) (b)

Figure 9. Parma inflow and uncorrupted observations: reference vs estimated inflow hydrograph (a) and observed vs modeled water levels (b). The residuals between reference and estimated values are also reported.

mation about the related effects, as illustrated by the increasing range of the 95% credibility interval. However, the estimated wave is inside the 95% credibility interval, thus confirming the good results of the solution.

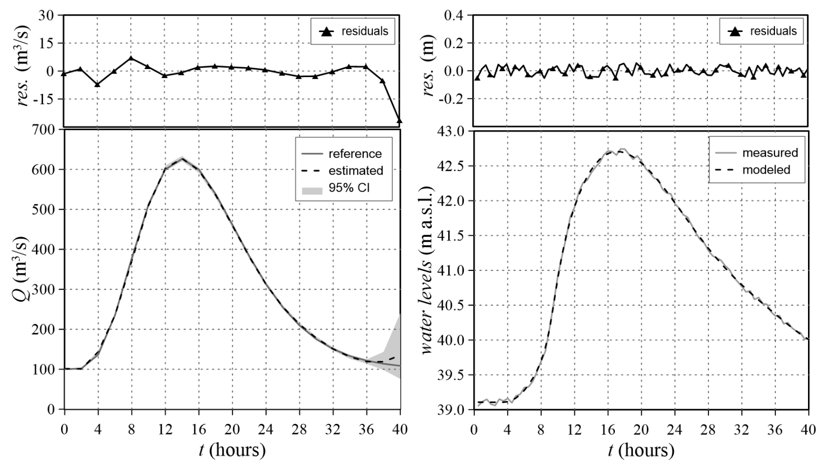

(a) (b)

Figure 10. Parma inflow and corrupted observations: reference vs estimated inflow hydrograph (a) and observed vs modeled water levels (b). The residuals between reference and estimated values are also reported.

The structural parameters estimated in presence and absence of corrupted observations are reported in Table 1.

Quantitative assessment of the methodology accuracy has been achieved by means of the Nash-Sutcliffe E_h, root mean square error RMSE and error in the peak discharge E_p values reported in Table 2. The E_h values are over the 99%, the E_p

Table 1. Parma inflow: initial and estimated structural parameters.

		No random errors	Random errors
σ_R^2 (m^2)	Initial	-	1.00E-4
	Estimated	-	1.09E-3
σ_S^2 (m^{6}s^{-2})	Initial	5.00E+2	5.00E+2
	Estimated	1.07E+3	5.36E+1
l(s)	Initial	6.48E+4	6.48E+4
	Estimated	2.90E+4	5.28E+4

ones are almost negligible and the RMSE error is less than 0.5 m^3/s without random errors and reaches the maximum value of 6 m^3/s with corrupted observations.

Table 2. Parma inflow: Nash-Sutcliffe E_h, root mean square error RMSE and error in the peak discharge E_p values.

	E_h (-)	RMSE (m^3/s)	E_p (%)
No random errors	99.99	0.49	-0.04
Random errors	99.88	6.65	0.15

4.2 Inflow hydrograph estimation on the Secchia River

The second test case concerns both a different river reach and shape of the inflow hydrograph. The studied domain includes a 25 km-long reach of the Secchia River (Northern Italy) between the flood control reservoir of Rubiera-Campogalliano located at West of Modena town (point A) and the gauging station of Ponte Bacchello (point C) and referring the water level observations to the gauging station of Ponte Alto (point B) (Fig. 11). The modeled river reach is characterized by the presence of many flood plains and floodable areas that influence the flood propagation. The bathymetry was derived from a 1 m resolution DTM obtained through a LiDAR survey carried out in drought condition.

The domain was discretized by means of a non-uniform BUQ grid (Vacondio et al. (2017)), resulting in $77 \cdot 10^3$ computing cells. The Manning roughness coefficient in the riverbed was assumed equal to 0.05 s/m$^{1/3}$ (Vacondio et al. (2016)).

The discharge hydrograph to be estimated is the synthetic flood wave of 20 years-return period of the Secchia River with a peak value of about 780 m^3/s after 18 hours. In order to increase the non-smoothness of the wave, a quite abrupt increment that separates the initial steady-state condition (100 m^3/s) from the rising limb was introduced (Fig. 12-a). It is noteworthy that this flow hydrograph is characterized by a pseudo real irregular shape, that cannot be approximated by a parametric function

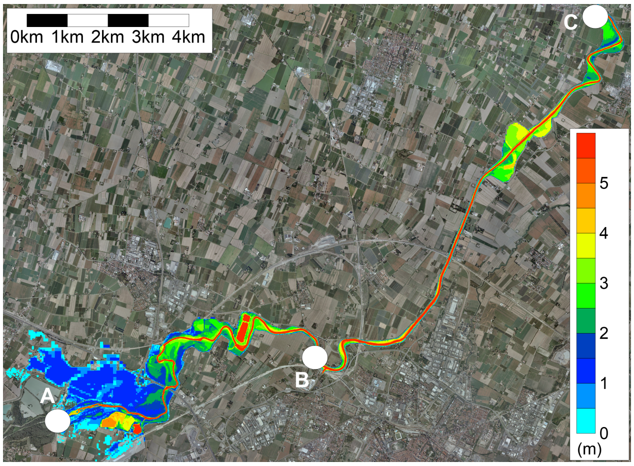

Figure 11. Map of the water depths at the flood pick occurrence on the Secchia river, with indicated the upstream (A) and downstream (C) boundary conditions and the intermediate observation site (B).

(i.e. Gamma distribution, Pearson function). The inflow hydrograph ended in 72 hours and it was discretized using 2 hours steps (N_p=37), whereas the observation stage hydrograph was discretized every 0.5 hours (144 water level values). The inflow hydrograph was firstly estimated assuming the water levels extracted in section B free of errors (with truncation error resulting in a variance of 10^{-8} m^2), and secondly considering corrupted observations with random errors uniformly distributed with maximum deviations of ± 0.05 m and variance 10^{-3} m^2 (Fig. 12-b). Besides the discharge and stage hydrographs, Fig. 12-a depicts the discharge hydrograph resulted in the downstream boundary condition section, in order to highlight the attenuation effect exerted by the flood plains and floodable areas.

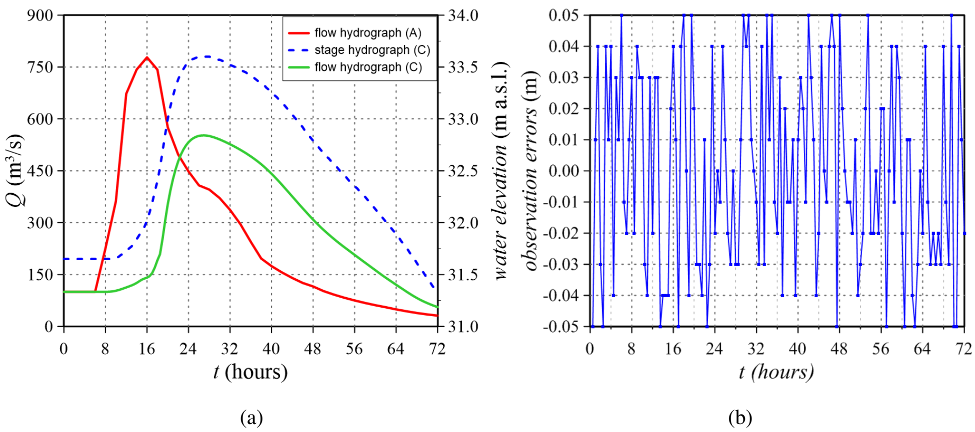

Figure 12. Secchia inflow: flow and stage hydrographs referred to sections A and C, respectively (a) and observation error distribution (b).

The parameters were estimated in a logarithmic space and their initial values were calculated adopting the linesearch tool of the bgaPEST (Fienen et al. (2013)). The prior pdf was described by means of a linear and Gaussian variogram, in the configuration with and without corrupted observations, respectively (Table 3). The initial model parameter values were calculated adopting the linesearch tool of the bgaPEST (Fienen et al. (2013)), and the estimation was performed in a logarithmic space. As shown in Fig. 13 for the simulation without corrupted observations, the estimated flood wave matches almost perfectly the reference one, as well as the modeled water levels agree with the measured ones. With reference to the peak value, the flood wave is estimated with less than the 0.03% difference against the reference one, and similarly, the residuals between modeled and observed water levels are less than the 0.01%.

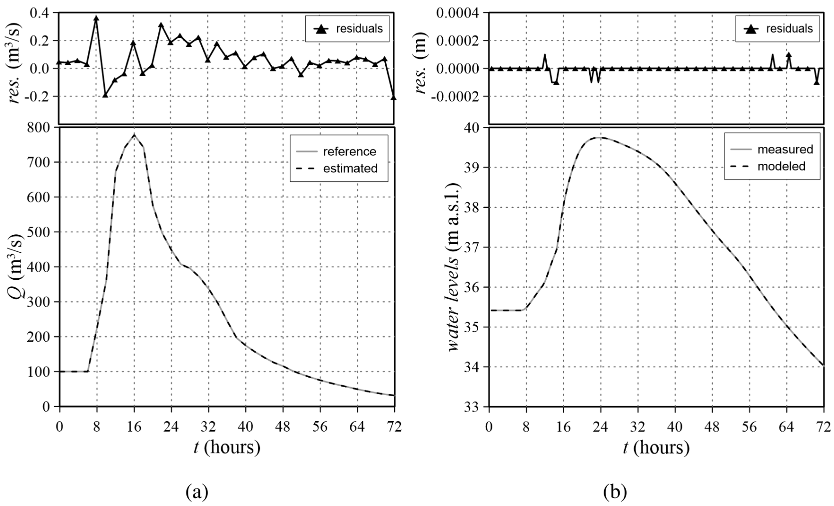

Figure 13. Secchia inflow and uncorrupted observations: reference vs estimated inflow hydrograph (a) and observed vs modeled water levels (b). The residuals between reference and estimated values are also reported.

The results of the simulation with corrupted observations depicted in Fig. 14 highlight that both the shape and the peak value are well captured. The residual between reference and estimated discharge, referred to the peak value, is about 8%, whereas the misfit between observed and modeled water levels is less than 0.3%. The small discrepancies of the estimated peak flood wave from the reference one are essentially caused by the fact that the portion with the peak is discretized with only a few parameters and the adopted variogram smooths the solution.

The structural parameters estimated in presence and absence of corrupted observations are reported in Table 3.

The resulted indicators used for evaluating the accuracy of the methodology are reported in Table 4. The Nash-Sutcliff efficiency E_h exceed the 99%, the errors in the peak flow E_p are almost negligible and the RMSE error is less than 1 m^3/s without random errors and reaches the maximum value of 16 m^3/s with corrupted observations: these values highlight the accuracy of the procedure in estimating the overall shape and peak of the inflow hydrographs.

With the aim of exemplifying the efficiency of the proposed parallel inverse procedure, some details about the computational times are furnished for this test case, whose main features are reported in Table 5.

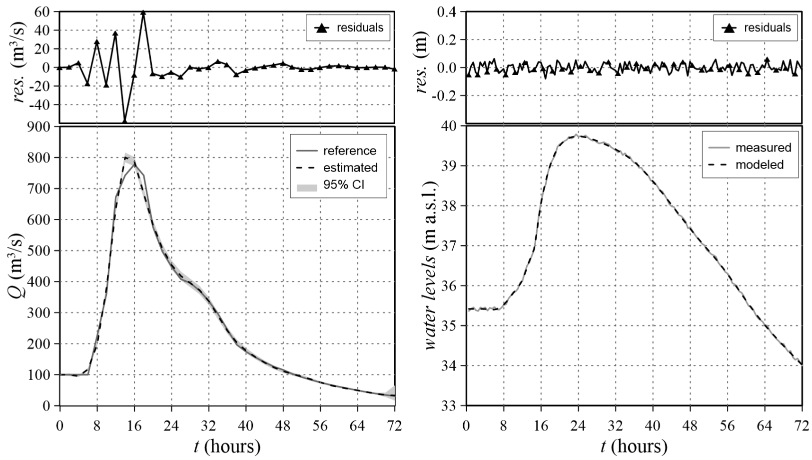

(a) (b)

Figure 14. Secchia inflow and corrupted observations: reference vs estimated inflow hydrograph (a) and observed vs modeled water levels (b). The residuals between reference and estimated values are also reported.

Table 3. Secchia inflow: initial and estimated structural parameters.

		No random errors	Random errors
θ ($m^6 s^{-3}$)	Initial	1.00E-10	-
	Estimated	3.97E-6	-
σ_R^2 (m^2)	Initial	-	1.00E-4
	Estimated	-	1.11E-3
σ_S^2 ($m^6 s^{-2}$)	Initial	-	5.00E+2
	Estimated	-	1.38E+1
l(s)	Initial	-	4.32E+4
	Estimated	-	3.88E+4

The computational time of the whole inflow hydrograph simulation (72 hours) is 9.62 minutes, whereas the simulations for evaluating the Jacobian matrix and testing parameters from 2 till 37 required a computational time progressively lower than 9.62 minutes, thanks to the restart option illustrated in the Sect. 3. In order to evaluate the total time required by the inverse procedure, it is noteworthy that dealing with an HPC cluster the global run time depends on the number of the available GPUs. However, this test was performed using 10 GPUs and the computational cost of the 609 runs was about 13 hours. Since the implemented procedure that manages the interaction between host and server can be used for different HPC cluster, the availability of a cluster equipped with N_p GPUs would have allowed the estimation of the flood wave in about 8 hours. On the

Table 4. Secchia inflow: Nash-Sutcliffe E_h, root mean square error RMSE and error in the peak discharge E_p values.

	E_h (-)	RMSE (m^3/s)	E_p (%)
No random errors	99.99	0.13	-0.02
Random errors	99.44	16.57	2.89

Table 5. Secchia inflow: characteristics of the simulation.

Number of parameters N_p	37
Physical total time of the inflow hydrograph	72 hours
Physical total time of the run testing the 1^{st} parameter p_1, assuming 100 hours for reaching the steady state condition	172 hours
Computational time of the whole inflow hydrograph simulation (72 hours)	9.62 minutes
Computational time of the run testing the 1^{st} parameter (172 hours)	19.38 minutes
Number of the BGA iterations N_i for the model parameter estimation	4
Number of the BGA iterations N_o for the structural parameter estimation	4
Total number of simulations N_t (Eq. 15)	609

other side, the adoption of the serial bgaPEST procedure and the PARFLOOD code as routing model would have required about 4 days of computations that means about 8 times slower than the parallel procedure here proposed. Particularly interesting is the hypothetical evaluation of the computational time for a serial BGA procedure and the adoption of a serial CPU code as forward hydraulic model. Vacondio et al. (2014) pointed out that the PARFLOOD code led to speedup up to two order of magnitude if compared to a serial CPU code. Therefore, if a serial BGA procedure and the GPU forward model would have required about 4 computational days, the inverse problem solution with a serial forward code would ended in 400 computational days, making the use of the inverse procedure practically unfeasible.

5 Reconstruction of a historical event: the December 2009 flood wave on the Secchia River

After the model validation assessed in the previous section, the inverse procedure is now adopted in the framework of a real field application, by investigating the December 2009 flooding event on the Secchia River, which is one of the three most significant events occurred in the last ten years in this river. The Interregional Agency for the Po River (AIPo) monitored the river and provided the water stage hydrographs recorded in two gauging stations, indicated in Fig. 11, with letters B and C, respectively. As shown in Fig. 15, the registered water levels present more than a rising and recession limb, and thus, beside

Hydrology and Earth System Sciences
Discussions
Open Access

the challenges related to a real field application, this test aims at addressing also the estimation of an inflow with two peaks. In order to estimate the discharge at section A (Fig. 11), the water levels registered at point B and C were assumed as observations and downstream boundary condition, respectively. The event was simulated from 9 p.m. of the 22^{nd} December 2009, till 12 a.m. of the 26^{th} December, for a total duration of 87 hours. The water levels were recorded every 0.5 hours, and thus the observations consist of 174 values. Conversely, the unknown inflow hydrograph was discretized every hour, in a result of 88 parameters to be estimated (N_p=88). The stage hydrographs, adopted as observations and downstream boundary condition, respectively, are shown in Fig. 15.

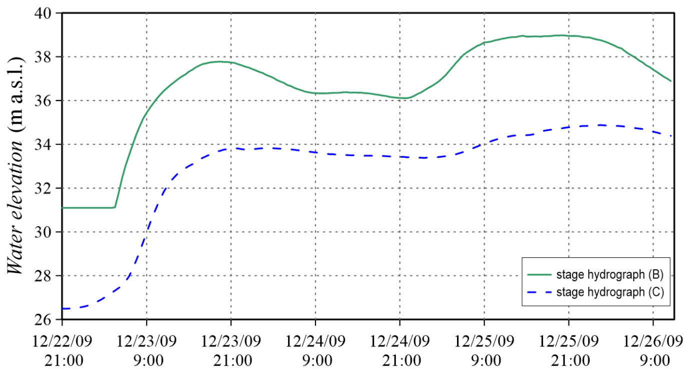

Figure 15. December 2009 registered stage hydrographs on the Secchia River, referred to sections B and C, respectively.

The studied domain is analogous to the one previously adopted for a syntethic inflow, and thus, the reader is kindly referred to Sect. 4.2 for the information about bathymetry, initial condition, and roughness configuration.

As before, the parameters were estimated in a logarithmic space and their initial values were calculated adopting the line-search tool of the bgaPEST (Fienen et al. (2013)). The prior pdf was described by means of a Gaussian variogram; the initial and estimated structural parameters are reported in Table 6.

Table 6. Secchia 2009 event: initial and estimated structural parameters.

	σ_S^2 (m^6s^{-2})	l(s)
Initial	5.00E+2	6.48E+4
Estimated	1.49E+1	3.36E+4

Figure 16 shows the estimated flood wave, which presents an irregular shape and two main peaks, as it could be expected from the observed stage hydrograph. Moreover, an additional small intermediate peak is captured that was not so evident from the registered water levels in Fig. 16, even if a local maximum can be seen around 3 p.m. of the 24^{th} December 2009. The resulted flood wave is included in the 95% credibility interval, and moreover the solution presents neither instabilities nor oscillations. During the computation, the variance of the epistemic error was assumed equal to 10^{-3} m^2; as shown in Sect. 4,

Hydrol. Earth Syst. Sci. Discuss., https://doi.org/10.5194/hess-2018-118
Manuscript under review for journal Hydrol. Earth Syst. Sci.
Discussion started: 27 April 2018

this means considering the observed water levels corrupted with random errors with maximum deviations of ±0.05 m. In Fig. 16, the flood wave estimated reducing the variance of half an order of magnitude is also depicted (dotted line): the solution appears slightly smoothed in a few points but substantially similar to the inflow resulting with the higher variance, which is thus considered as the estimated inflow of the studied event. The comparison between modeled and measured water levels is presented in Fig. 17: it is relevant to notice that the residuals between the two trends are mostly less than 2 cm and only in a few points of the first rising limb they reach the highest value of 18 cm. This real field application further confirms the capability of the proposed inverse procedure of estimating irregular inflow hydrographs in real rivers.

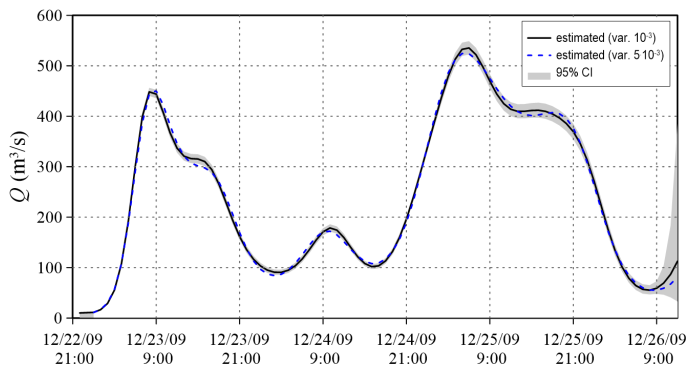

Figure 16. Secchia 2009 event: estimated inflow hydrographs assuming the epistemic variance equal to 10^{-3} m^2 and $5{\cdot}10^{-3}$ m^2, respectively.

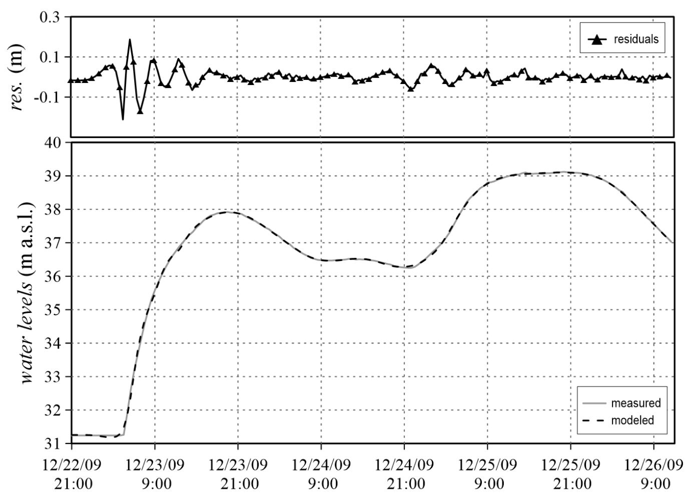

Figure 17. Secchia 2009 event: observed vs modeled water levels. The residuals between reference and estimated values are also reported.

6 Conclusions

In this work the inverse problem of estimating the unknown inflow hydrograph in an upstream-ungauged section, having water level information only in downstream sites has been solved by means of a Bayesian methodology. The key aspects in the solution of this problem have been the adoption of a parallel 2D-SWE code running on GPUs and the performance of the simulations over a HPC cluster. The parallelization of the runs useful for the Jacobian matrix computation and the implementation of an *ad hoc* procedure, which allows taking advantage of any HPC cluster with GPUs, by means of the protocol SSH, have provided a remarkable reduction of the computational costs: the more GPUs are available on the cluster, the less time is required for the parameter estimation. For a considered case, this parallel procedure reduced the computational time of a factor 8 against running the 2D-SWE code on a single GPU. Furthermore, the analysis of the runtimes has highlighted that the use of a parallel hydraulic forward routing model is the *sine qua non* for solving this type of inverse problem, whereas the adoption of a serial code would lead to inadmissible computational times. The inverse procedure has been validated considering two different natural rivers; in both tests, no instabilities, due to the adopted inverse procedure or to the availability of a stable, fast and accurate forward hydraulic model, arose. Moreover, the obtained results have highlighted that the implemented procedure well estimates the unknown inflow hydrographs with different and irregular shapes and in presence of corrupted observations: quantitative indicators have proved the accuracy of the methodology. In all the presented tests, the resulted Nash-Sutcliff efficiency criterion exceeded the 99%, the error in the peak discharge was less than 3% and the RMSE error less than 2%. Finally, the proposed inverse procedure allowed the estimation a historical flood wave characterized by the presence of two peaks, without reaching instabilities in the solution. Future development of the methodology will focus on the possibility of reconstructing the flood waves also in presence of levee breaches and flooding outside the river region.

Competing interests. The authors declare that they have no conflict of interest.

Acknowledgements. This work was partially supported by Ministry of Education, Universities and Research under the Scientific Independence of young Researchers project, grant number RBSI14R1GP, CUP code D92I15000190001. This research benefits from the HPC (High Performance Computing) facility of the University of Parma, Italy. Interregional Agency for the Po River (AIPo) is also gratefully acknowledged for providing data.

References

Beven, K. J.: Rainfall-runoff modelling: the primer, John Wiley & Sons, 2011.

Bruen, M. and Dooge, J.: Harmonic analysis of the stability of reverse routing in channels, Hydrology and Earth System Sciences, 11, 559–568, 2007.

Butera, I., Tanda, M. G., and Zanini, A.: Simultaneous identification of the pollutant release history and the source location in groundwater by means of a geostatistical approach, Stochastic Environmental Research and Risk Assessment, 27, 1269–1280, 2013.

Das, A.: Reverse stream flow routing by using Muskingum models, Sadhana, 34, 483–499, 2009.

Doherty, J. E.: PEST, Model-Independent Parameter Estimation – User Manual,sixth ed., Tech. rep., Watermark Numerical Computing, Brisbane, Australia, 2016.

Dooge, J. and Bruen, M.: Problems in reverse routing, Acta Geophysica Polonica, 53, 357, 2005.

D'Oria, M. and Tanda, M. G.: Reverse flow routing in open channels: A Bayesian Geostatistical Approach, Journal of hydrology, 460, 130–135, 2012.

D'Oria, M., Mignosa, P., and Tanda, M. G.: Bayesian estimation of inflow hydrographs in ungauged sites of multiple reach systems, Advances in Water Resources, 63, 143–151, 2014.

D'Oria, M., Mignosa, P., and Tanda, M. G.: An inverse method to estimate the flow through a levee breach, Advances in Water Resources, 82, 166–175, 2015.

Eli, R., Wiggert, J., and Contractor, D.: Reverse flow routing by the implicit method, Water Resources Research, 10, 597–600, 1974.

Fienen, M., Hunt, R., Krabbenhoft, D., and Clemo, T.: Obtaining parsimonious hydraulic conductivity fields using head and transport observations: A Bayesian geostatistical parameter estimation approach, Water resources research, 45, 2009.

Fienen, M. N., Clemo, T., and Kitanidis, P. K.: An interactive Bayesian geostatistical inverse protocol for hydraulic tomography, Water Resources Research, 44, 2008.

Fienen, M. N., D'Oria, M., Doherty, J. E., and Hunt, R. J.: Approaches in highly parameterized inversion: bgaPEST, a Bayesian geostatistical approach implementation with PEST: documentation and instructions, Tech. rep., US Geological Survey, 2013.

Glickman, M. E. and Van Dyk, D. A.: Basic bayesian methods, Topics in Biostatistics, pp. 319–338, 2007.

Hoeksema, R. J. and Kitanidis, P. K.: An application of the geostatistical approach to the inverse problem in two-dimensional groundwater modeling, Water Resources Research, 20, 1003–1020, 1984.

Kitanidis, P. K.: Quasi-linear geostatistical theory for inversing, Water Resources Research, 31, 1995.

Kitanidis, P. K. and Vomvoris, E. G.: A geostatistical approach to the inverse problem in groundwater modeling (steady state) and one-dimensional simulations, Water resources research, 19, 677–690, 1983.

Koussis, A., Mazi, K., Lykoudis, S., and Argiriou, A.: Reverse flood routing with the inverted Muskingum storage routing scheme, Natural Hazards and Earth System Sciences, 12, 217, 2012.

Koussis, A. D. and Mazi, K.: Reverse flood and pollution routing with the lag-and-route model, Hydrological Sciences Journal, 61, 1952–1966, 2016.

Leonhardt, G., D'Oria, M., Kleidorfer, M., and Rauch, W.: Estimating inflow to a combined sewer overflow structure with storage tank in real time: evaluation of different approaches, Water Science and Technology, 70, 1143–1151, 2014.

Michalak, A. M. and Kitanidis, P. K.: A method for enforcing parameter nonnegativity in Bayesian inverse problems with an application to contaminant source identification, Water Resources Research, 39, 2003.

Michalak, A. M., Bruhwiler, L., and Tans, P. P.: A geostatistical approach to surface flux estimation of atmospheric trace gases, Journal of Geophysical Research: Atmospheres, 109, 2004.

Nash, J. E. and Sutcliffe, J. V.: River flow forecasting through conceptual models part I—A discussion of principles, Journal of hydrology, 10, 282–290, 1970.

Saghafian, B., Jannaty, M., and Ezami, N.: Inverse hydrograph routing optimization model based on the kinematic wave approach, Engineering Optimization, 47, 1031–1042, 2015.

Snodgrass, M. F. and Kitanidis, P. K.: A geostatistical approach to contaminant source identification, Water Resources Research, 33, 537–546, 1997.

Szymkiewicz, R.: Solution of the inverse problem for the Saint Venant equations, Journal of Hydrology, 147, 105–120, 1993.

Vacondio, R., Dal Palù, A., and Mignosa, P.: GPU-enhanced finite volume shallow water solver for fast flood simulations, Environmental modelling & software, 57, 60–75, 2014.

Vacondio, R., Aureli, F., Ferrari, A., Mignosa, P., and Dal Palù, A.: Simulation of the January 2014 flood on the Secchia River using a fast and high-resolution 2D parallel shallow-water numerical scheme, Natural Hazards, 80, 103–125, 2016.

Vacondio, R., Palù, A. D., Ferrari, A., Mignosa, P., Aureli, F., and Dazzi, S.: A non-uniform efficient grid type for GPU-parallel Shallow Water Equations models, Environmental Modelling & Software, 88, 119 – 137, 2017.

Zucco, G., Tayfur, G., and Moramarco, T.: Reverse flood routing in natural channels using genetic algorithm, Water resources management, 29, 4241–4267, 2015.